Research Square

Preprints are preliminary reports that have not undergone peer review.
They should not be considered conclusive, used to inform clinical practice,
or referenced by the media as validated information.

Choroid plexus volume in relation to volumetric and susceptibility characteristics of white matter hyperintensities in metabolic syndrome: a two-cohort MRI study

Xinxin Huo
Shandong Provincial Hospital
Linfeng Yang
Shandong Maternal and Child Health Hospital
Zhenyu Cheng
Shandong Medical And Pharmaceutical University
Boyao Chen
Shandong Provincial Hospital
Fushuai Zhang
Shandong Medical And Pharmaceutical University
Yiwen Chen
Shandong Provincial Hospital
Pengcheng Liang
Shandong Provincial Hospital
Nan Zhang
Shandong Provincial Hospital
Yena Che
Shandong Provincial Hospital
Jiaxiang Xin
Siemens Healthineers
Changhu Liang
Shandong Provincial Hospital
Lingfei Guo
glfsci@163.com

Shandong Provincial Hospital
Li Feng
Shandong Provincial Hospital
Meng Li

Jena University Hospital

Research Article

Keywords: Metabolic syndrome, White matter hyperintensity, Choroid plexus, Quantitative susceptibility mapping, Cross-cohort analysis

Posted Date: September 3rd, 2026

DOI: https://doi.org/10.21203/rs.3.rs-10473506/v1

License: This work is licensed under a Creative Commons Attribution 4.0 International License.
Read Full License

Additional Declarations: No competing interests reported.

Abstract

Aims This study aims to explore the pathophysiological links among MetS, choroid plexus (CP), and white matter hyperintensities (WMHs) to clarify mechanisms of cognitive decline in MetS.

Methods A total of 133 participants from the Jinan cohort and 5,594 from the UK Biobank (UKB) were included. In Jinan, a three-way interaction (CP volume × WMH susceptibility × MetS) was modeled for WMH volume. Multivariate regression, restricted cubic spline, and generalized estimating equations assessed CP-WMH associations. Mediation analyses evaluated whether WMH mediated links between MetS severity and cognitive domains. In the UKB, serial mediation analyses using structural equation models were performed to test the directional cascade from triglyceride-glucose (TyG) index to cognitive domains.

Results CP volume correlated with WMH characteristics across both cohorts. In Jinan, the association of CP and WMH was significant only in MetS individuals with elevated WMH susceptibility. Longitudinally, CP volume showed a time-varying negative association with WMH susceptibility. In the UKB, both total WMH and periventricular hyperintensity (PVH) volume increased with CP over time. WMH volume was linked to poorer processing speed and global cognition and mediated the association between MetS severity and cognition in the UKB. And significant indirect effects of TyG on global cognition via CP and WMH volume was found in the UKB.

Conclusion MetS was associated with CP enlargement and WMH abnormalities across two cohorts. These imaging characteristics were further associated with poorer processing speed and global cognitive performance.

1. Introduction

With an increasing global prevalence, metabolic syndrome (MetS) is estimated to affect more than one billion people worldwide and is associated with end-organ damage in the cardiovascular, gastrointestinal, renal, and nervous systems, particularly at advanced stages[1,2]. Critically, MetS and its components, particularly obesity characteristics, accelerate brain aging by separate mechanisms and contribute to cognitive impairment and neurodegeneration[3,4]. White matter hyperintensities (WMHs) are regarded as punctate or confluent high-signal regions on fluid-attenuated inversion recovery (FLAIR) sequences, and are usually divided into periventricular (PVH) and deep (DWMH) types[5]. WMH reflects chronic cerebral hypoperfusion. This pathological process leads to axonal loss, demyelination and gliosis, and is closely associated with cognitive dysfunction and a high risk of stroke[6–8]. Recent research has confirmed that hypertension and metabolic abnormalities are strongly related to WMHs[9]. At the same time, the crucial role of cerebrospinal fluid (CSF) homeostasis in maintaining the integrity of the white matter has also been confirmed[10]. The choroid plexus (CP) is a bridge connecting the peripheral and central nervous systems. Besides contributing to the production of numerous neuroprotective and developmental proteins, its enlargement has been interpreted as the activation of neuroinflammation

and disruption of brain homeostasis, especially under the condition of increased blood–brain barrier (BBB) permeability[11,12]. Structural and functional abnormalities in CP have been implicated in the pathophysiological mechanisms of neurodegenerative diseases, finally leading to cognitive impairment[13]. Recent studies have suggested that increased CP volume may serve as an indicator of cognitive decline in patients with mild cognitive impairment (MCI)[14]. So it has been hypothesized that in the context of MetS, this change is more likely to be the driving forces that promote the neurodegenerative pathological process. A retrospective investigation has indicated that enlarged CP may cause dysfunction of the glymphatic system, thereby driving the progression of white matter hyperintensities[15]. This finding has subsequently raised a deeper question of whether changes in CP reflect MetS severity by affecting the microstructure integrity of white matter.

The progression of WMHs has been commonly observed in populations with neurocognitive disorders, and the intrinsic abnormalities in the white matter microstructure have been further confirmed to be a key factor in impairing its connectivity with the cortical regions[16]. It is largely insufficient to observe changes in the microscopic structure relying on changes in WMH volume. Advances in traditional contrast weightings, quantitative susceptibility mapping (QSM) demonstrates a superior contrast to-noise ratio (CNR), reflecting highly detailed anatomical mapping of brain and accurately recognize and track alteration of cerebral tissue[17]. Therefore, integrating volume measurements and magnetic susceptibility parameters is expected to clarify the microstructural pathological mechanism of white matter lesions, providing a new approach for detecting dementia in preclinical stage before volume changes occur.

Moreover, WMH volume has been proposed to be a key mediator linking diverse metabolic factors to cognitive decline. A study indicated that the PVH may specifically increase an individual's susceptibility to cognitive impairment related to hypertension, particularly in nonverbal memory and executive function[18]. The current studies confirmed the mediating role of the total WMH volume in the relationship between the between MetS severity and cognitive function in a small sample[19]. Notably, insulin resistance (IR) is considered one of the key driving mechanisms for the occurrence and development of WMH. It directly damages the white matter microstructure through pathways such as endothelial dysfunction, oxidative stress, and inflammatory response[20]. However, the MetS scores may not fully capture the continuous spectrum of metabolic burden. The triglyceride-glucose (TyG) index, as a simple and effective marker for insulin resistance, provides a continuous measurement of metabolic risk and has been proven to be independently associated with the progression of WMH[21]. This has prompted an exploration of the intrinsic connection between MetS and its related indicators, microstructure and macroscopic distribution of WMH, and multiple cognitive functions.

In this study, we leveraged both the Jinan cohort and the UK Biobank (UKB) to test whether metabolic burden exerts a directional influence on the relationship among CP volume, WMH characteristics, and cognitive function. To test this hypothesis, we first explored the association between CP volume and WMH characteristics in the two cohorts. Moreover, the WMH characteristics from the two cohorts were

leveraged to examine the internal relationship between MetS and cognitive performance. Finally, We built serial mediation models in the UKB to test the directional cascade from metabolic dysfunction to cognitive impairment via CP and WMH. By integrating multimodal neuroimaging and cross-cohort validation, this study investigates the potential pathophysiological relevance of CP and WMH interactions in MetS, with implications for both neurodegenerative and cerebrovascular mechanisms.

2. Methods

2.1 Study population

Subjects for this research were obtained from two prospective cohorts: the UKB (https://www.ukbiobank.ac.uk) based in the United Kingdom, and the Jinan cohort (ISRCTN13222678) based in China. Figure 1 shows a flow chart with the inclusion and exclusion criteria of the two cohorts, and the detailed procedure of the criteria is provided in the **supplementary materials, Section 1**. Ultimately, a total of 133 participants (63 healthy controls and 70 MetS patients) from the Jinan cohort and 5,594 participants (2,771 healthy controls and 2,823 MetS patients) from the UKB, all with comprehensive blood parameters and cognitive function, were included in this study. Propensity score matching were uesd in UKB between groups (see **Supplementary materials, Section 1**). Another 23 subjects from the Jinan cohort and 572 subjects from the UKB with complete follow-up data were included in the longitudinal study. We adopted the Chinese Medical Association Diabetes Branch (CDS) criteria[22] to diagnose MetS in the Jinan cohort and the National Cholesterol Education Program Adult Treatment Panel III (NCEP–ATP III)[23] in the UKB. The specific diagnostic criteria can be found in the **supplementary materials, Section 2**.

2.2 Image acquisition and measurements

Subjects from the Jinan cohort underwent three-dimensional T1-weighted imaging (3D-T1WI) on a 3.0-T MR system (MAGNETOM Skyra, Siemens Healthcare, Erlangen, Germany) with a 32-channel head coil. 3D-T1W images were acquired via the following parameters: TR/TE = 2500 ms/2.35 ms; scan matrix = 256 × 256; FOV= 240 × 240 mm^2; flip angle = 8°; and voxel size = 0.9 × 0.9 × 0.9 mm^3. A three-dimensional multiecho gradient-echo (3D ME-GRE) sequence was performed with TR/TE = 50 ms/6.8 ms; TE interval = 4.1 ms; number of echoes = 10; flip angle = 15°; and voxel size = 1 × 1 × 2 mm^3. In addition, T2-weighted turbo spin echo and T2-FLAIR images were acquired during scanning to ensure that the subjects had no brain lesions. The subjects remained still and conscious, breathing quietly during the scanning. The specific scanning parameters from the UKB can be found in the **supplementary materials**, Section 3.1.

2.3 Image postprocessing

For the extraction of the imaging features in the Jinan cohort, structural MRI data were preprocessed via fMRIPrep 20.1.1, which generated a nonlinear deformation field to normalize individual native images to

the MNI2009c standard space. The segmentation of WMH was performed with an optimized algorithm based on multidimensional gated recurrent units (GRUs), incorporating data augmentation, selective sampling, residual learning, and DropConnect regularization within the RNN state[24] **(Figure S1)**.

On the basis of a deep learning algorithm, the CP volume of 636 subjects on 3D-T1WI was automatically segmented by leveraging 3D nnU-Net. ITK-SNAP software was used to delineate the region of the CP in the lateral ventricles of several subjects by two experienced radiologists (with 7 and 20 years of experience). We randomly selected 236 cases to train the model, and the remaining 400 cases were utilized for testing this model (Dice score = 0.8, $P < 0.001$). After segmentation, the output results were processed by Dr. Li to refine the segmented CP regions. The detailed postprocessing steps of UKB are provided in the **supplementary materials**, Section 3.1.

2.4 Clinical assessment

Basic clinical characteristics, including age, sex, education, smoking status, drinking status and components of metabolic syndrome, were collected from the Jinan cohort. Metabolism-related blood biochemical data were obtained from each subject via a harmonized venous sampling procedure. Various neuropsychological tests, including the Stroop Color and Word Test (SCWT)[25], Trail Making Test (TMT)[26], Auditory Verbal Learning Test (AVLT)[27], and Symbol Digit Modalities Test (SDMT)[28], were subsequently administered. All tests were conducted by professionals in a quiet, stationary setting. Each test was z-transformed individually for participants, and global cognition was determined as the mean z score of all domains (processing speed, executive function, memory)[9,18,29,30]. The processing speed is z transformed from the SDMT and TMT (Part A); the executive function is z transformed from the TMT (Part B) and SCWT; and the memory is z transformed from the AVLT. Additional details on the basic clinical data of the UKB can be found in the **supplementary materials**, Section 3.2.

2.5 Statistical analyses

Demographic, lifestyle, socioeconomic, image feature, and cognitive domain differences were evaluated in both cohorts via independent *t* tests and chi-square tests between individuals with MetS and HCs. Mann–Whitney U tests were applied for nonnormally distributed data, predominantly within the Jinan cohort. In all subsequent analyses, the measurements of CP volume and WMH volume were adjusted for estimated total intracranial volume (eTIV). Multiple linear regression analyses were performed to explore the associations between CP volume and white matter hyperintensity characteristics in both the MetS group and the total sample. In the Jinan cohort, the models were adjusted for age, sex, years of education, smoking status, alcohol consumption, and lateral ventricle volume (LVV). For validation in the UKB, additional covariates, including ethnic background and the Townsend deprivation index, were also incorporated. The three-way interaction term (CP volume × WMH susceptibility × MetS) was included in the multiple linear regression models as a predictor of WMH volume adjusted for age, sex, years of education, and LVV in the Jinan cohort. Continuous predictors in the interaction models were mean-centered to alleviate multicollinearity. Simple-slope analysis was conducted to probe the conditional effects of CP volume on WMH volume at varying levels of WMH susceptibility across MetS statuses.

Restricted cubic spline (RCS) models were used to visualize the relationship between CP volume and WMH characteristics in the subgroups. Subgroup analyses were performed to explore the associations of CP volume with WMH volume in different groups from the UKB. Additionally, generalized estimating equations were used to investigate the associations between CP volume and WMH characteristics adjusted for follow-up time and several covariates across the two cohorts in the longitudinal exploration. Linear regression analyses and mediation analyses were used to explore the relationships among WMH volume, cognitive domains, and MetS in the Jinan cohort and UKB cohort, respectively. In the UKB, we also built a structural equation model (SEM) using the lavaan package in R Studio. The model included direct paths from TyG index to cognitive domains, with all paths adjusted for age, sex, educational levels, ethnicity, smoking, alcohol, and Townsend deprivation index. Bootstrapping (1,000 resamples) was used to obtain bias corrected confidence intervals for the indirect effects. All the statistical results were analyzed via SPSS version 27.0 software (SPSS Inc., Chicago, IL, USA) and R Studio software (v2023.06.2), with $P < 0.05$ considered statistically significant. The flowcharts were created with BioGDP.com[31].

3. Results

3.1 Baseline characteristics and group comparisons

Subjects in both cohorts were categorized as HCs or MetS patients on the basis of diagnostic criteria. Table 1 and **Table S1** display the demographic details, clinical characteristics, and cognitive domains of each group at baseline in the Jinan cohort and UKB, respectively. Metabolic markers were assessed at the UKB baseline, while the brain images analyzed in this study were obtained an average of 8.8 ± 1.7 years later, with all other indicators aligning with the imaging features. In the Jinan cohort, the MetS group was older, had a lower proportion of females, had a higher percentage of current smokers, and consumed alcohol. Comparisons of the imaging features of the Jinan cohort revealed prominent differences in CP volume ($P < 0.001$), WMH volume ($P = 0.001$), WMH susceptibility ($P = 0.038$), and LVV ($P = 0.041$) between these two groups. Comparisons of the imaging features of UKB also revealed prominent differences in CP volume ($P < 0.001$), total WMH volume ($P < 0.001$), DWMH volume ($P < 0.001$), PVH volume ($P < 0.001$) and LVV ($P = 0.003$) between these two groups. The prevalence of MetS components and cognitive domains (except for executive function in the UKB) showed significant differences, whereas no significant differences between groups were found for eTIV. Baseline assessment in the UKB can be found in the **supplementary materials**, Section 3.3.

Table 1
Baseline characteristics of the two groups in Jinan cohort.

Characteristic	Mets(n = 70)	HCs(n = 63)	χ^2/t/Z	*P* value
Age (years), median (IQR)	60 (53, 67)	53.5 (48, 59)	-3.286	0.001[a]
Sex, Female N (%)	23 (32.8)	40 (63.4)	12.482	< 0.001[χ2]
Education (years), median (IQR)	12 (12, 15)	16 (12, 16)	-3.824	< 0.001[a]
Smoking, [yes, N (%)]	27 (42.9%)	7 (11.1%)	11.740	< 0.001[χ2]
Alcohol drinking, [yes, N (%)]	33 (52.4%)	16 (25.4%)	5.850	0.016[χ2]
Metabolic syndrome, N (%)				
Hypertension, [yes, N (%)]	58 (82.9%)	13 (20.6%)	51.586	< 0.001[χ2]
Hyperglycemia, [yes,N (%)]	65 (103.2%)	14 (22.2%)	65.700	< 0.001[χ2]
Obesity, [yes,N (%)]	58 (92.1%)	22 (34.9%)	29.820	< 0.001[χ2]
Reduced HDL, [yes,N (%)]	12 (17.1%)	0 (0.0%)	10.040	< 0.001[χ2]
Elevated triglycerides, [yes,N (%)]	48 (76.2%)	10 (15.9%)	36.390	< 0.001[χ2]
Neuropsychological assessments[#]				
Memory, mean (± SD)	-0.27 (1.02)	0.29 (0.90)	3.346	0.001[t#]
Processing Speed, mean (± SD)	-0.32 (0.99)	0.35 (0.68)	4.483	< 0.001[t#]
Executive Function, mean (± SD)	-0.35 (1.06)	0.38 (0.46)	5.203	< 0.001[t#]
Global Cognition, mean (± SD)	-0.30 (0.85)	0.34(0.56)	5.174	< 0.001[t#]
Image features				

[χ2] Chi-square test; [t] two independent sample *t* test; [a] Mann–Whitney U test;

[*]Plasma biomarkers were log-transformed and standardized to z scores.

[#]Each neuropsychological tests were z-transformed separately for all participants and global cognition was defined as mean z score of all cognitive domains, the FDR (False Discovery Rate) method was used for result correction.

Abbreviations: Mets, metabolic syndrome; HCs, healthy controls; HDL, high-density lipoprotein; CP volume, choroid plexus volume; eTIV, estimated total intracranial volume; WMH, White matter hyperintensity; LVV, lateral ventricle volume; SD, Standard Deviation; IQR, Inter Quartile Range.

Characteristic	Mets(n = 70)	HCs(n = 63)	χ^2/t/Z	*P* value
CP volume[$mm^3 \times 10^3$, median (IQR)]	1.40 (1.20, 1.78)	1.15 (0.89, 1.42)	-3.893	< 0.001[a]
WMH volume[$mm^3 \times 10^2$, median (IQR)]	10.87(4.50, 38.14)	5.58 (2.37, 13.33)	-3.177	0.001[a]
eTIV, [$mm^3 \times 10^5$, mean (± SD)]	14.89 (1.62)	14.71 (1.15)	0.736	0.463[t]
LVV, [$mm^3 \times 10^4$, mean (± SD)]	2.35 (1.18)	1.95 (1.02)	−2.065	0.041[t]
Mean QSM WMH [ppb × 10^{-9}, mean (± SD)]	−13.06 (8.86)	−16.43 (9.46)	2.095	0.038[t]
χ^2 Chi-square test; *t* two independent sample *t* test; [a] Mann–Whitney U test;				
*Plasma biomarkers were log-transformed and standardized to z scores.				
#Each neuropsychological tests were z-transformed separately for all participants and global cognition was defined as mean z score of all cognitive domains, the FDR (False Discovery Rate) method was used for result correction.				
Abbreviations: Mets, metabolic syndrome; HCs, healthy controls; HDL, high-density lipoprotein; CP volume, choroid plexus volume; eTIV, estimated total intracranial volume; WMH, White matter hyperintensity; LVV, lateral ventricle volume; SD, Standard Deviation; IQR, Inter Quartile Range.				

3.2 Relationship between WMH characteristics and CP volume

Three regression models were established to explore the relationships between WMH characteristics and CP volume across the two cohorts. **Table S2** shows that CP volume was significantly correlated with WMH susceptibility in MetS (Model 3: β = -0.941, *P* = 0.045) and general subjects (Model 3: β = -0.915, *P* = 0.008) after full adjustment in the Jinan cohort. Although the correlation between CP volume and WMH volume was not significant in the Jinan cohort, the interaction effects among CP volume, MetS status and WMH susceptibility were observed for WMH volume (β = 0.271, *P* = 0.019) (Fig. 2a and **Table S3-4**). Simple-slope analysis revealed that the association between CP volume and WMH volume was not significant in the HC group, whereas in the MetS group, the positive effect of CP on WMH became significant when WMH susceptibility exceeded one standard deviation (β = 4.900, *P* = 0.004), indicating that elevated WMH susceptibility amplifies the positive association between CP volume and WMH volume, specifically in MetS patients (Fig. 2b and **Table S5**). In addition, CP volume was significantly correlated with total WMH volume and PVH volume in MetS patients after full adjustment in UKB, whereas no significant correlation was found between CP volume and DWMH volume (Fig. 2c, d and **Table S6**). RCS analysis, subgroup analysis and longitudinal analysis are presented in the **supplementary materials, Section 4, Figure S2-3, and Table S7-12**.

3.3 WMH volume and cognitive domains

The correlations between the results of the cognitive domain and WMH volume across the two cohorts are shown in Fig. 3. The results revealed that increased WMH volume in the Jinan cohort was strongly negatively correlated with processing speed (β = -0.288, *P* = 0.014) and global cognition (β = -0.317, *P* = 0.008) after adjusting for age, sex and years of education **(**Fig. 3a, b**)**. We also discovered the mediating role of WMH volume between MetS severity and cognitive domains after adjusting for age, sex, education level, and ethnic background in the UKB. Total WMH, PVH, and DWMH partially mediated the relationship between the MetS score and processing speed, with the mediating effect accounting for 17.9%, 17%, and 12.5% of the total effect, respectively. Total WMH, PVH, and DWMH partially mediated the relationship between the MetS score and global cognition, with the mediating effect accounting for 11.9%, 11.1%, and 9.21% of the total effect, respectively **(**Fig. 3c**)**. The detailed statistical results are shown in **Tables S13-15**.

3.4 Serial mediation analysis in the UKB

As presented in Fig. 4, all path coefficients were statistically significant except the direct effect of TyG index on global cognition. TyG index was positively associated with CP volume (β = 0.039, *P* = 0.001). CP volume was positively associated with total WMH volume (β = 0.181, *P* < 0.001). TyG also had a direct positive effect on WMH volume (β = 0.075, *P* < 0.001). Higher WMH volume was negatively associated with global cognition (β = -0.074, *P* < 0.001). This serial indirect effect was significant (β = -0.001 *P* = 0.007) **(**Fig. 4a**)**. Moreover, identical results were obtained when PVH volume was used as the mediator **(**Fig. 4b**)**. The serial indirect effect was not significant when the DWMH act as the mediator. Results for processing speed, executive function, and memory are provided in **Table S16-18.**

4. Discussion

This prospective, dual-cohort study was conducted to examine associations between CP volume, WMH characteristics, and multiple cognitive domains in individuals with MetS, using integrated cross-sectional and longitudinal approaches. In the Jinan cohort, interaction effects among CP volume, WMH susceptibility, and WMH volume were evaluated, and nonlinear relationships between CP volume and WMH susceptibility were assessed in certain subgroups. The association between CP volume and WMH volume was more pronounced in individuals with MetS than in HCs, and higher WMH susceptibility values may reinforce this association, indicating that microstructural alterations in WMHs may precede volumetric changes. In the UK Biobank, association between CP volume and the distribution of WMH volume were examined, especially PVH volume and total WMH volume. Longitudinal associations between CP volume and WMH characteristics were observed in both cohorts. Furthermore, WMH volume in both cohorts was closely associated with global cognition and processing speed across cognitive domains. In the larger population, WMH volume was observed to mediate the association between MetS severity and cognitive performance. And serial mediation analyses also revealed that TyG index affects cognitive function through a cascade of CP enlargement and WMH accumulation. In the

context of MetS, systemic metabolic disorders may initially impair the function of the CP, subsequently disrupt white matter microstructure, consequently lead to macroscopic accumulation of white matter damage (increased WMH volume), and ultimately impair cognitive function.

The observed relationship between CP and WMH characteristics may reflect a pathophysiological mechanism involving impaired CSF dynamics and neuroinflammation in MetS patients. The progression of MetS has been closely associated with the activation of multiple inflammatory signaling pathways and the release of various proinflammatory cytokines[32]. Specifically, studies in animal models have revealed that peripheral immune activation can trigger an intracerebral inflammatory cascade reaction originating from the CP. The enlargement of the CP volume is not only regarded as a sign of central neuroinflammation and decreased CSF clearance capacity, but it is also one of the possible mechanisms contributing to white matter damage[33]. In clinical neuroinflammatory diseases such as multiple sclerosis, the pathological changes in CP have been given more specific clinical significance. CP enlargement has been associated with increased neuroinflammation and impaired white matter repair, particularly in periventricular regions detected by positron emission tomography (PET) imaging[34,35]. Recent multi-omics analyses have further identified common peripheral pathways that suggest enhanced immune stress in individual patients with WMHs[36,37]. Based on this, a reasonable hypothesis is that the systemic inflammation, oxidative stress, and endothelial dysfunction in MetS may increase CP permeability, disrupt the CSF homeostasis, and thereby promote the accumulation of neurotoxic and pro-inflammatory molecules in the periventricular white matter. These systematic pathological process can precisely explain the significant findings of the UKB study, indicating that the PVH exhibits unique susceptibility to pathological effects in CP.

In the mechanism of white matter damage, microglial degeneration related to ferroptosis is a key factor, which achieves this by driving iron-mediated oxidative stress and lipid metabolic dysfunction[38]. In this context, the QSM technique can non-invasively capture the corresponding changes in tissue magnetic susceptibility. Susceptibility values in the basal ganglia predominantly reflects elevated iron deposition, whereas it increased in the white matter may result from increased iron accumulation, demyelination, or both[39]. A systematic review by Ravanfar et al. further demonstrated that QSM consistently reveals heightened magnetic susceptibility in brain regions vulnerable to neurodegenerative processes, including AD and Parkinson's disease (PD)[40]. Among subjects with MetS and elevated WMH susceptibility values, a significant correlation between the CP volume and the WMH volume was observed, indicating that susceptibility measures capture subtle white matter alterations not detected by conventional volumetric assessments. In the longitudinal study, CP volume had no significant influence on WMH volume in the Jinan cohort, whereas its association with WMH susceptibility remained notable. These finding indicated that WMH susceptibility might be a more sensitive indicator for reflecting the MetS progression than WMH volume.

The research conducted by the UKB indicates that MetS severity is not only correlated with the total WMH volume, but also significantly correlated with multiple cognitive domains such as memory,

reasoning, and processing speed[9]. PVH, rather than the DWMH, have been implicated in linking systolic blood pressure to cognitive performance, particularly in the domains of nonverbal memory and executive function[18]. Therefore, we combined the two cohorts and discovered that WMH volume was associated with cognitive performance, particularly processing speed and global function. WMH volume was observed to mediate the association between MetS severity and cognitive domains, and in the UKB, PVH showed a stronger mediating effect than DWMH, supporting that metabolic factors may accelerate the neurodegenerative processes underlying cognitive impairment. The underlying reason is likely that MetS can induce central insulin resistance (IR), which suppresses the activation of genes related to cholinergic neuron function, memory, cognition, and synaptic plasticity[16]. Importantly, peripheral insulin resistance, as a core component of MetS, may lead to central IR, and central IR is closely linked to the progression of neurodegenerative disorders[32]. To directly quantify peripheral insulin resistance, we further constructed a serial mediation model using the TyG index as the exposure (TyG → CP → WMH → cognitive function). This analysis revealed a significant serial indirect effect which confirmed that insulin resistance may affects cognitive function through a cascade of CP enlargement and WMH accumulation. Additionally, brain IR also triggers tau protein hyperphosphorylation and neurofibrillary tangles (NFTs), which can distort cholinergic neurotransmission and result in cognitive impairment. Hormonal imbalance and neuroinflammation in MetS patients also enhance the neuropathology of Alzheimer's disease (AD) by inducing mitochondrial dysfunction and oxidative stress[16]. Other neurological diseases causing neurodegeneration may likewise be associated with WMHs and cognitive decline[32].

Several aspects of our study should be improved. First, although the dual-cohort design combining the Jinan and UK Biobank cohorts enhances generalizability, differences in demographic and imaging characteristics may introduce heterogeneity. Second, MetS status was determined at baseline, and neuroimaging and cognitive outcomes were evaluated years later in the UKB. Third, residual confounding from unmeasured metabolic, vascular, or lifestyle factors remains possible, as with all observational designs. Additionally, both cohorts are subject to selection bias, particularly the UK Biobank, in which participants are generally healthier than the wider population, which may lead to underestimation of effect sizes. Future research should aim to integrate CSF and PET biomarkers to clarify the mechanistic relevance of WMH characteristics in neuroinflammation and protein clearance. In parallel, larger and multicenter cohorts are warranted to further advance the translational potential of WMH markers in predicting cognitive decline and informing early intervention strategies in MetS patients.

5. Conclusion

Overall, our dual-cohort study demonstrated that metabolic abnormity may drive cognitive decline through a cascade initiated by CP enlargement, followed by microstructural destruction in white matter, the accumulation of macroscopic WMH volume enlargement and, ultimately, disrupts processing speed and global cognition.

Declarations

Ethics approval

All procedures performed in studies involving human participants were in accordance with the ethical standards of the institutional and national research committee and with the 1964 Helsinki Declaration and its later amendments or comparable ethical standards. The study was approved by the Ethics Review Board of Shandong Provincial Hospital Affiliated with Shandong First Medical University (NO. 2024 – 398) and the Ethical approval for the UKB (ref.11/NW/0382).

Clinical trial number

This study made use of the UK Biobank Resource (Application 147766) and the study procedures were approved by the Ethical Committee of the Institutional Review Board (IRB) of Shandong Institute of Medical Imaging (2019-002).

Consent for publication

Informed consent was obtained from all individual participants included in the study.

Competing interests

The authors declare that they have no competing interests.

Abbreviations

Mets, metabolic syndrome; HCs, healthy controls; MRI, Magnetic Resonance Imaging.

Abbreviations: MetS, metabolic syndrome; CP volume, choroid plexus volume;

PVH, periventricular hyperintensities; WMH, white matter hyperintensity; LVV, lateral ventricle volume; eTIV, estimated total intracranial volume.

Abbreviations: MetS, metabolic syndrome;

DWMH, deep white matter hyperintensities; PVH, periventricular hyperintensities; WMH, white matter hyperintensity.

Abbreviations: Mets, metabolic syndrome;

WMH, white matter hyperintensities; PVH, periventricular hyperintensities; TyG index, triglyceride-glucose index.

Funding

This work was supported by grants from the Key R&D Program of Shandong Province, China (2025CXPT106, 2025CXGC020305), the Natural Science Foundation of Shandong Province (ZR2020MH288, ZR2024MH026), the Technology Development Plan of Jinan (202328066), the Medical and Health Science, Technology Development Project of Shandong Province (202309010557, 202309010560, 202409010479).

Acknowledgments

We are sincerely grateful to all volunteers from the Jinan cohort and UK Biobank, as well as the clinical and data teams who supported recruitment, imaging, and follow-up. This study made use of the UK Biobank Resource (Application 147766). We also thank the investigators and staff maintaining the Jinan cohort for their dedicated contributions. We sincerely thank Dr. Yuan Cao for her invaluable contributions to developing the automated choroid plexus segmentation pipeline, which significantly enhanced the accuracy of our methodology.

Disclosure

Availability of data and material

The study subjects were all from the cohort independently established by our team: Clinical trial number: ISRCTN13222678. Some or all datasets generated during and/or analyzed during the current study are not publicly available but are available from the corresponding author on reasonable request.

References

1. Kalisz K, Navin PJ, Itani M, Agarwal AK, Venkatesh SK, Rajiah PS. Multimodality Imaging in Metabolic Syndrome: State-of-the-Art Review. Radiographics. 2024;44(3). 10.1148/rg.230083.
2. Saklayen MG. The Global Epidemic of the Metabolic Syndrome. Curr Hypertens Rep. 2018;20(2). 10.1007/s11906-018-0812-z.
3. Huang S-H, Chen S-C, Geng J-H, Wu D-W, Li C-H. Metabolic Syndrome and High-Obesity-Related Indices Are Associated with Poor Cognitive Function in a Large Taiwanese Population Study Older than 60 Years. Nutrients. 2022;14(8). 10.3390/nu14081535.
4. Shen C, Liu C, Qiu A. Metabolism-related brain morphology accelerates aging and predicts neurodegenerative diseases and stroke: a UK Biobank study. Translational psychiatry Jun.

2023;29(1):233. 10.1038/s41398-023-02515-1.

5. Wardlaw JM, Smith EE, Biessels GJ, et al. Neuroimaging standards for research into small vessel disease and its contribution to ageing and neurodegeneration. The Lancet Neurology Aug. 2013;12(8):822–38. 10.1016/s1474-4422(13)70124-8.
6. Bachmann D, von Rickenbach B, Buchmann A, et al. White matter hyperintensity patterns: associations with comorbidities, amyloid, and cognition. Alzheimer's Res & therapy Apr. 2024;1(1):67. 10.1186/s13195-024-01435-6.
7. Lee M, Suh CH, Sohn JH, et al. Impact of white matter hyperintensity volumes estimated by automated methods using deep learning on stroke outcomes in small vessel occlusion stroke. Front Aging Neurosci. 2024;16:1399457. 10.3389/fnagi.2024.1399457.
8. Oveisgharan S, Yu L, Poole VN, et al. Association of White Matter Hyperintensities With Pathology and Progression of Parkinsonism in Aging. JAMA neurology Dec. 2021;1(12):1494–502. 10.1001/jamaneurol.2021.3996.
9. Qureshi D, Topiwala A, Al Abid SU, Allen NE, Kuźma E, Littlejohns TJ. Association of Metabolic Syndrome With Neuroimaging and Cognitive Outcomes in the UK Biobank. Diabetes care Aug. 2024;1(8):1415–23. 10.2337/dc24-0537.
10. Lun MP, Monuki ES, Lehtinen MK. Development and functions of the choroid plexus-cerebrospinal fluid system. Nature reviews Neuroscience Aug. 2015;16(8):445–57. 10.1038/nrn3921.
11. Althubaity N, Schubert J, Martins D, et al. Choroid plexus enlargement is associated with neuroinflammation and reduction of blood brain barrier permeability in depression. NeuroImage: Clin. 2022;33doi. 10.1016/j.nicl.2021.102926.
12. Saunders NR, Dziegielewska KM, Fame RM, Lehtinen MK, Liddelow SA. The choroid plexus: a missing link in our understanding of brain development and function. Physiol Rev. 2023;103(1):919–56. 10.1152/physrev.00060.2021.
13. Čarna M, Onyango IG, Katina S, et al. Pathogenesis of Alzheimer's disease: Involvement of the choroid plexus. Alzheimer's & dementia: J Alzheimer's Association Aug. 2023;19(8):3537–54. 10.1002/alz.12970.
14. Jiang J, Zhuo Z, Wang A, et al. Choroid plexus volume as a novel candidate neuroimaging marker of the Alzheimer's continuum. Alzheimer's Res & therapy Jul. 2024;3(1):149. 10.1186/s13195-024-01520-w.
15. Li Y, Zhou Y, Zhong W, et al. Choroid Plexus Enlargement Exacerbates White Matter Hyperintensity Growth through Glymphatic Impairment. Annals neurology Jul. 2023;94(1):182–95. 10.1002/ana.26648.
16. Garnier-Crussard A, Cotton F, Krolak-Salmon P, Chételat G. White matter hyperintensities in Alzheimer's disease: Beyond vascular contribution. Alzheimer's & dementia: J Alzheimer's Association Aug. 2023;19(8):3738–48. 10.1002/alz.13057.
17. Ruetten PPR, Gillard JH, Graves MJ. Introduction to Quantitative Susceptibility Mapping and Susceptibility Weighted Imaging. The Br J radiology Sep. 2019;92(1101):20181016.

10.1259/bjr.20181016.

18. Gronewold J, Jokisch M, Schramm S, et al. Periventricular rather than deep white matter hyperintensities mediate effects of hypertension on cognitive performance in the population-based 1000BRAINS study. Journal hypertension Dec. 2022;1(12):2413–22. 10.1097/hjh.0000000000003270.
19. Zheng W, Zhou X, Yin J, et al. Metabolic syndrome-related cognitive impairment with white matter hyperintensities and functional network analysis. Obesity (Silver Spring Md) Oct. 2023;31(10):2557–67. 10.1002/oby.23873.
20. Sun J, Xu B, Zhang X, et al. The Mechanisms of Type 2 Diabetes-Related White Matter Intensities: A Review. Front public health. 2020;8:498056. 10.3389/fpubh.2020.498056.
21. Nam KW, Kwon HM, Jeong HY, Park JH, Kwon H, Jeong SM. High triglyceride-glucose index is associated with subclinical cerebral small vessel disease in a healthy population: a cross-sectional study. Cardiovascular diabetology May. 2020;6(1):53. 10.1186/s12933-020-01031-6.
22. Wang X, Yang F, Bots ML, et al. Prevalence of the Metabolic Syndrome Among Employees in Northeast China. Chinese Med journal Aug. 2015;5(15):1989–93. 10.4103/0366-6999.161337.
23. Neeland IJ, Lim S, Tchernof A, et al. Metabolic syndrome. *Nature reviews Disease primers*. Oct. 2024;17(1):77. 10.1038/s41572-024-00563-5.
24. Esteban O, Markiewicz CJ, Blair RW, et al. fMRIPrep: a robust preprocessing pipeline for functional MRI. Nature methods Jan. 2019;16(1):111–6. 10.1038/s41592-018-0235-4.
25. Scarpina F, Tagini S. The Stroop Color and Word Test. Front Psychol. 2017;8:557. 10.3389/fpsyg.2017.00557.
26. Llinàs-Reglà J, Vilalta-Franch J, López-Pousa S, Calvó-Perxas L, Torrents Rodas D, Garre-Olmo J. The Trail Making Test. Assessment Mar. 2017;24(2):183–96. 10.1177/1073191115602552.
27. Conde-Blanco E, Pariente JC, Carreño M, et al. Testing an Adapted Auditory Verbal Learning Test Paradigm for fMRI to Lateralize Verbal Memory in Patients with Epilepsy. AJNR Am J neuroradiology Oct. 2022;43(10):1445–52. 10.3174/ajnr.A7622.
28. Benedict RH, Smerbeck A. Mar. Construct validity of the symbol-digit modalities test. *Multiple sclerosis (Houndmills, Basingstoke, England)*. 2023;29(3):483–485. 10.1177/13524585221112381
29. Lezak MD, Howieson DB, Bigler ED, Tranel D. Neuropsychological assessment. 5th ed. Oxford University Press; 2012.
30. Strauss E, Sherman EMS, Spreen O. A compendium of neuropsychological tests: Administration, norms, and commentary. 3rd ed. Oxford University Press; 2006.
31. Jiang S, Li H, Zhang L, et al. Generic Diagramming Platform (GDP): a comprehensive database of high-quality biomedical graphics. Nucleic acids research Jan. 2025;6(D1):D1670–6. 10.1093/nar/gkae973.
32. Al-Kuraishy HM, Jabir MS, Albuhadily AK, Al-Gareeb AI, Rafeeq MF. The link between metabolic syndrome and Alzheimer disease: A mutual relationship and long rigorous investigation. Ageing Res

Rev Nov. 2023;91:102084. 10.1016/j.arr.2023.102084.

33. Liang P, Li M, Chen Y, et al. Associations of choroid plexus volume with white matter hyperintensity volume and susceptibility and plasma amyloid markers in cerebral small vessel disease. Alzheimer's Res & therapy Apr. 2025;23(1):90. 10.1186/s13195-025-01740-8.
34. Liu Z, Pardini M, Yaldizli Ö, et al. Magnetization transfer ratio measures in normal-appearing white matter show periventricular gradient abnormalities in multiple sclerosis. Brain: J neurology May. 2015;138(Pt 5):1239–46. 10.1093/brain/awv065.
35. Ricigliano VAG, Morena E, Colombi A, et al. Choroid Plexus Enlargement in Inflammatory Multiple Sclerosis: 3.0-T MRI and Translocator Protein PET Evaluation. Radiology Oct. 2021;301(1):166–77. 10.1148/radiol.2021204426.
36. Jickling GC, Ander BP, Zhan X, et al. Progression of cerebral white matter hyperintensities is related to leucocyte gene expression. Brain: J neurology Sep. 2022;14(9):3179–86. 10.1093/brain/awac107.
37. Yang Y, Knol MJ, Wang R, et al. Epigenetic and integrative cross-omics analyses of cerebral white matter hyperintensities on MRI. Brain: J neurology Feb. 2023;13(2):492–506. 10.1093/brain/awac290.
38. Adeniyi PA, Gong X, MacGregor E, et al. Ferroptosis of Microglia in Aging Human White Matter Injury. Annals neurology Dec. 2023;94(6):1048–66. 10.1002/ana.26770.
39. Ficiarà E, Stura I, Guiot C. Iron Deposition in Brain: Does Aging Matter? International J Mol sciences Sep. 2022;2(17). 10.3390/ijms231710018.
40. Ravanfar P, Loi SM, Syeda WT, et al. Systematic Review: Quantitative Susceptibility Mapping (QSM) of Brain Iron Profile in Neurodegenerative Diseases. Front NeuroSci. 2021;15:618435. 10.3389/fnins.2021.618435.

Figures

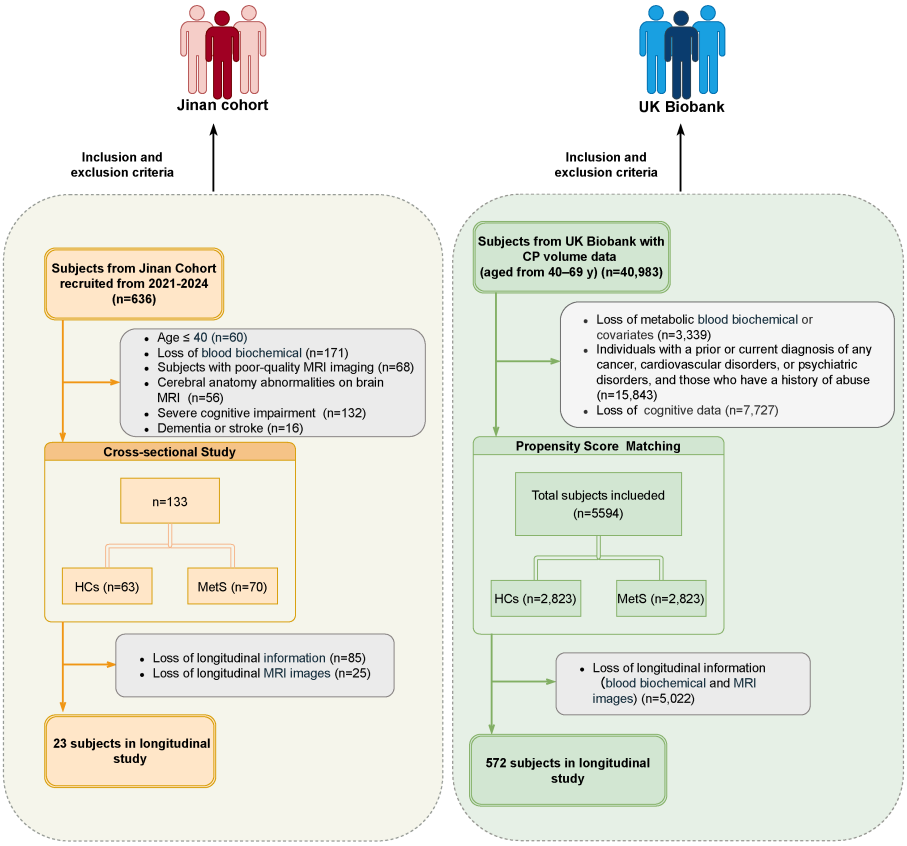


Figure 1

Participants inclusion/exclusion criteria in both two cohorts.

Abbreviations: Mets, metabolic syndrome; HCs, healthy controls; MRI, Magnetic Resonance Imaging.

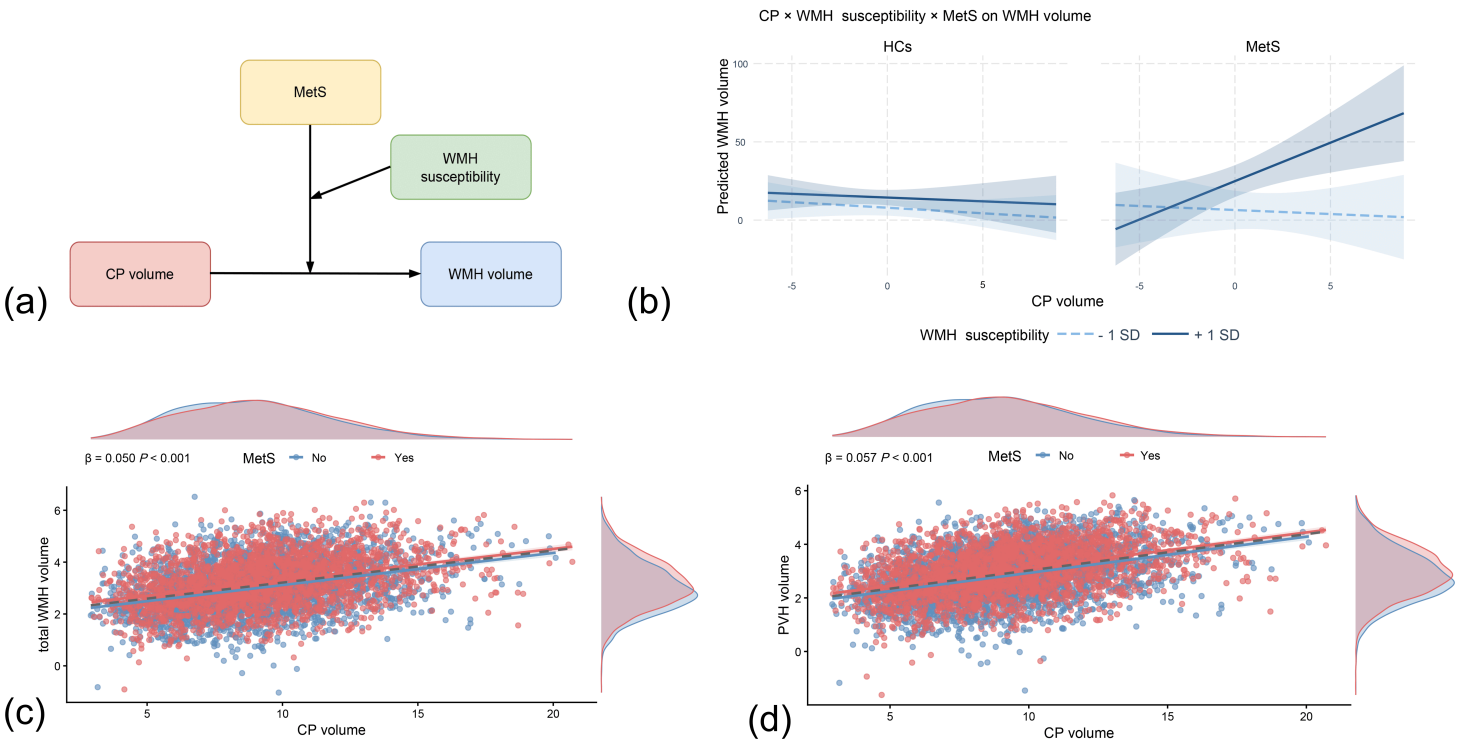


Figure 2

WMH characteristics associated with CP volume and across two cohorts in cross-sectional study.

(a) The three-way interaction (CP volume × WMH susceptibility × MetS) significantly predicted WMH volume in Jinan cohort controlling for sex, age, education, and LVV. **(b)** Simple slopes analyses revealed that higher WMH susceptibility strengthens the positive association between CP volume and WMH volume in MetS.**(c, d)** Association between CP volume and WMH volume (total WMH and PVH) in UKB adjusted for sex, age, education levels, smoking, alcohol drinking, ethnic background, Townsend deprivation index, and LVV. All the CP volume and WMH volume were corrected for the eTIV and then multiplied by 10^5.

Abbreviations: MetS, metabolic syndrome; CP volume, choroid plexus volume; PVH, periventricular hyperintensities; WMH, white matter hyperintensity; LVV, lateral ventricle volume; eTIV, estimated total intracranial volume.

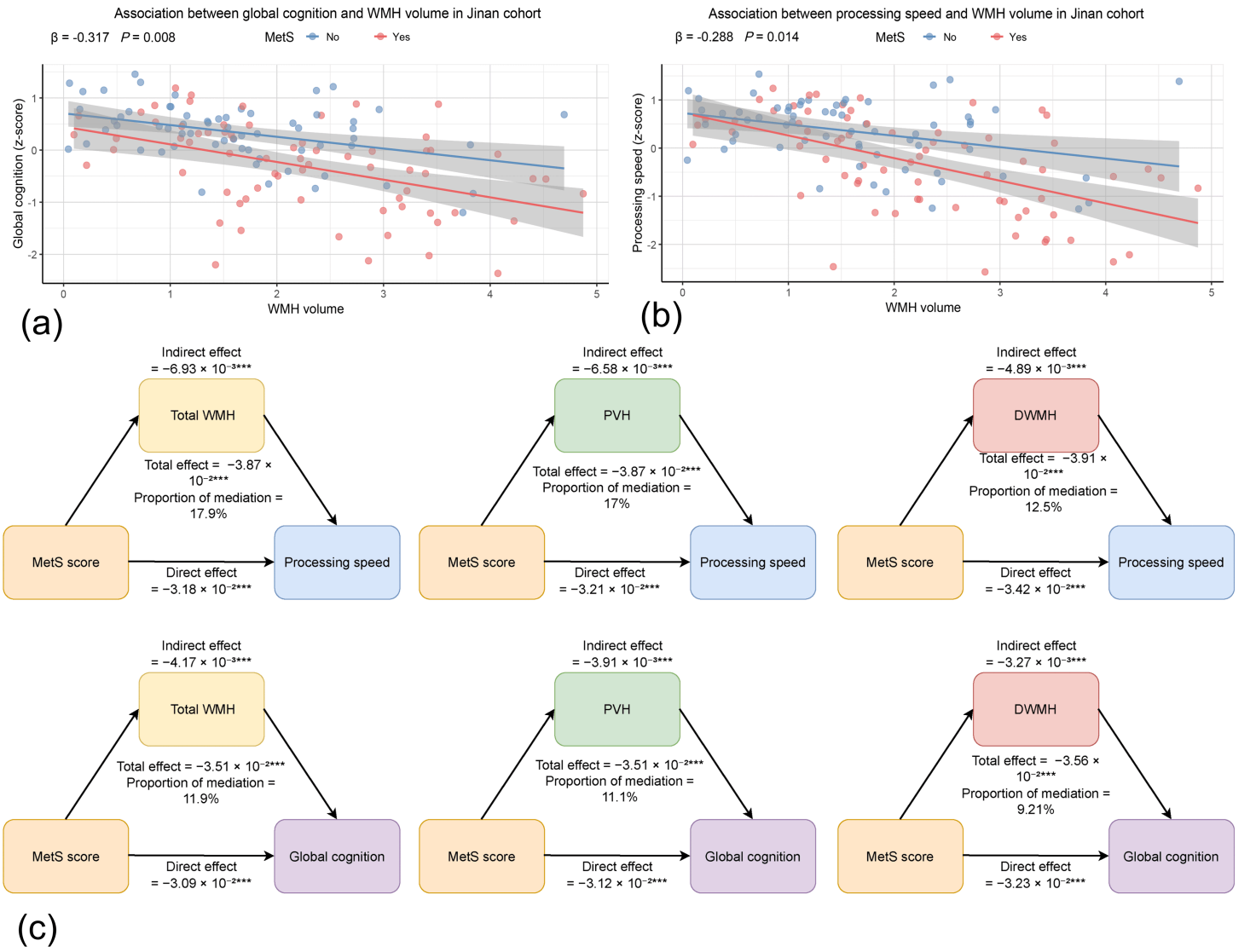


Figure 3

Relationship of WMH volume and multiple cognitive domains across two cohorts.

(a, b) Association between WMH volume and cognitive domains (global cognition and processing speed) in Jinan cohort adjusted for sex, age, and years of education. **(c)** Partial mediation effects of total WMH volume, PVH, and DWMH on the association between MetS score and cognitive domains (global cognition and processing speed). All the mediation analyses were adjusted for sex, age, education levels, and ethnic background and the FDR (False Discovery Rate) method was used for results.

Abbreviations: MetS, metabolic syndrome; DWMH, deep white matter hyperintensities; PVH, periventricular hyperintensities; WMH, white matter hyperintensity.

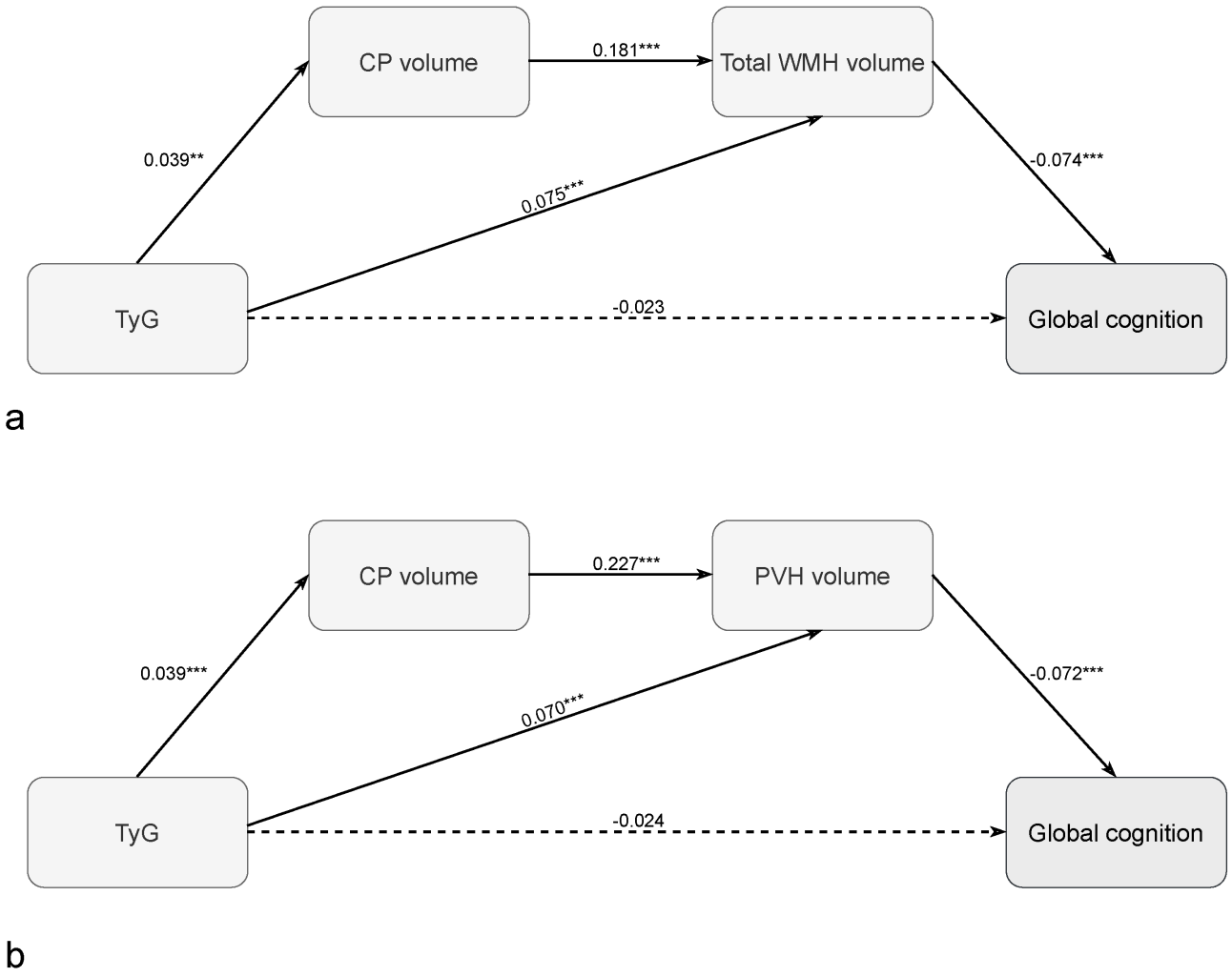


Figure 4

Standardized path coefficients of the serial mediation model. The model showed excellent fit: χ^2= 0.046, p = 0.830; CFI = 1.000; RMSEA = 0.000; SRMR = 0.000. **(a)** Standardized path coefficients of the serial mediation model using total WMH volume as the second mediator. **(b)** Standardized path coefficients of the serial mediation model using PVH volume as the second mediator. All models adjusted for age, sex, ethnicity, smoking, alcohol, education, and Townsend deprivation index. Only significant paths are shown (*P*< 0.05). Dashed line indicates non-significant direct effect.

***P* < 0.01, ****P* < 0.001.

Abbreviations: Mets, metabolic syndrome; WMH, white matter hyperintensities; PVH, periventricular hyperintensities; TyG index, triglyceride-glucose index.

Supplementary Files

This is a list of supplementary files associated with this preprint. Click to download.

- Supplementarymaterial.docx